Supplementary Methods

Capture-based sequencing

RNA capture probes for the coding regions of the 69 genes were designed using Agilent's SureDesign service (https:// earray.chem.agilent.com/suredesign/home.htm). Pooled and barcoded libraries for NGS were prepared using SureSelect QXT kits (Agilent Technologies, Santa Clara, California), according to the manufacturer's protocol. Prepared libraries were sequenced by 150-bp SE reads using Illumina MiSeq sequencers. Filtering of candidate variants was achieved, as described previously [1]. We first excluded single nucleotide variants (SNVs) with allele frequencies of >0.01 in any population within the Exome Aggregation Consortium [2] (ExAC: http://exac.broadinstitute.org); National Heart, Lung, and Blood Institute Exome Sequencing Project exome variant server dataset ESP6500 (http://evs.gs.washington.edu/EVS/); 1000 Genomes catalog [3] (http://browser.1000genomes.org/index.html); Human Genetic Variation Database [4] (HGVD: http://www.genome. med.kyoto-u.ac.jp/SnpDB/); or the genome cohort study of Tohoku Medical Megabank Organization [5] (ToMMo: https://ijgvd.megabank. tohoku.ac.jp). We excluded SNVs with “LOW” impact severities, based on the definition in the GEMINI software [6]; these included the following functional predictions: “synonymous_coding,”

"intergenic," "upstream," "UTR," "intron," etc. To interpret the significance of the variants, we used the Polyphen2 [7], SIFT [8], CADD [9], MCAP [10], and GERP conservation scores [11]. The literature that was available in the Human Gene Mutation Database Pro [12] was reviewed to assess current evidence on the pathogenicity of previously reported variants. The detailed methods were described in our previous reports [13,14].

Supplementary Methods References

1. Chong JX, Burrage LC, Beck AE *et al.* Autosomal-Dominant Multiple Pterygium Syndrome Is Caused by Mutations in MYH3. *Am J Hum Genet* 2015; **96**: 841–849.

2. Lek M, Karczewski KJ, Minikel E V. *et al.* Analysis of protein-coding genetic variation in 60,706 humans. *Nature* 2016; **536**: 285–291.

3. 1000 Genomes Project Consortium, Auton A, Brooks LD *et al.* A global reference for human genetic variation. *Nature* 2015; **526**: 68–74.

4. Higasa K, Miyake N, Yoshimura J *et al.* Human genetic variation database, a reference database of genetic variations in the Japanese population. *J Hum Genet* 2016; **61**: 547–53.

5. Nagasaki M, Yasuda J, Katsuoka F *et al.* Rare variant discovery by deep whole-genome sequencing of 1,070 Japanese individuals. *Nat Commun* 2015; **6**: 8018.

6. Paila U, Chapman BA, Kirchner R *et al.* GEMINI: Integrative Exploration of Genetic Variation and Genome Annotations. *PLoS Comput Biol* 2013; **9**: e1003153.

7. Adzhubei IA, Schmidt S, Peshkin L *et al.* A method and server for predicting damaging missense mutations. *Nat Methods* 2010; **7**: 248–249.

8. Kumar P, Henikoff S, Ng PC. Predicting the effects of coding non-synonymous variants on protein function using the SIFT algorithm. *Nat Protoc* 2009; **4**: 1073–1082.

9. Kircher M, Witten DM, Jain P *et al.* A general framework for estimating the relative pathogenicity of human genetic variants. *Nat Genet* 2014; **46**: 310–315.

10. Jagadeesh KA, Wenger AM, Berger MJ *et al.* M-CAP eliminates a majority of variants of uncertain significance in clinical exomes at high sensitivity. *Nat Genet* 2016; **48**: 1581–1586.

11. Davydov E V., Goode DL, Sirota M *et al.* Identifying a high fraction of the human genome to be under selective constraint using GERP++. *PLoS Comput Biol* 2010; **6**: e1001025.

12. Stenson PD, Mort M, Ball E V. *et al.* The Human Gene Mutation Database: towards a comprehensive repository of inherited mutation data for medical research, genetic diagnosis and next-generation sequencing studies. *Hum Genet* 2017; **136**: 665–677.

13. Mori T, Hosomichi K, Chiga M *et al.* Comprehensive genetic testing approach for major inherited kidney diseases, using next-generation sequencing with a custom panel. *Clin Exp Nephrol* 2017; **21**: 63–75.

14. Fujimaru T, Mori T, Sekine A *et al.* Kidney enlargement and multiple liver cyst formation implicate mutations in PKD1/2 in adult sporadic polycystic kidney disease. *Clin Genet* 2018; **94**: 125–131.

Supplementary Table S1. Disease categories and the targeted genes included in this panel

Disease family	Targeted Gene
ADPKD	*PKD1, PKD2*
ARPKD	*PKHD1*
NPHP	*NPHP1, INVS, NPHP3, NPHP4, IQCB1, CEP290, GLIS2, RPGRIP1L, NEK8, SDCCAG8, TMEM67, TTC21B, WDR19, ZNF423, CEP164, ANKS6, IFT172, CEP83, DCDC2, XPNPEP3, SLC41A1*
JBS	*NPHP1, CEP290, RPGRIP1L, TMEM67, TTC21B, ZNF423, CEP164, IFT172, INPP5E, TMEM216, AHI1, ARL13B, CC2D2A, OFD1, KIF7, TCTN1, TMEM237, CEP41, TMEM138, C5orf42, TCTN3, TMEM231, CSPP1, PDE6D, MKS1, TCTN2, B9D1*
MKS	*NPHP3, CEP290, RPGRIP1L, TMEM67, TMEM216, CC2D2A, TMEM231, MKS1, TCTN2, B9D1, B9D2*
SLS	*NPHP1, INVS, NPHP3, NPHP4, IQCB1, CEP290, GLIS2, SDCCAG8, WDR19, CEP164*
BBS	*CEP290, SDCCAG8, TMEM67, TTC21B, WDR19, IFT172, MKS1, BBS1, BBS2, ARL6, BBS4, BBS5, MKKS, BBS7, TTC8, BBS9, BBS10, TRIM32, BBS12, WDPCP, BBIP1, IFT27, CCDC28B*
Skeletal ciliopathies	*TTC21B, WDR19, IFT172, WDR35, IFT122, IFT140, IFT43*
ADTKD	*MUC1, UMOD, HNF1B*
Others	*ASS1, NOTCH2*

ADPKD, autosomal dominant polycystic kidney disease; ARPKD, autosomal recessive polycystic kidney disease; NPHP, nephronophthisis; JBS, Joubert syndrome; MKS, Meckel syndrome; SLS, Senior–Løken syndrome; BBS, Bardet–Biedl syndrome; IFT, intraflagellar transport; ADTKD, autosomal dominant tubulointerstitial kidney disease

Supplementary Table S2. Primer sequences of *NPHP1*

Amplified Region [a]	Primer	Sequence	Product size (bp)	Annealing Temperature (ºC)
Exon 1	Forward	GCCGGTTGGTTTCCCTG	209	60
	Reverse	TAGGTGGGGTCACGGTGG		
Exon 10	Forward	GGCATTTTGGAAGTGCCTG	258	60
	Reverse	TTGCAACTATGACAAAATCTGG		
Exon 20	Forward	TCCTACCTCTTAGGTGGCTTTTAG	509	60
	Reverse	AATCGTGGAGGATCCATCTG		

[a] The following NCBI reference sequences were used: *NPHP1*, NM_000272.3

Supplementary Table S3. Detected copy number variants in *NPHP1*

Patient	Chromosome	Start [a]	End [a]	Gene	Gain/Loss
883	2	g.110879716	g.110962709	*NPHP1*	loss
896	2	g.110962410	g.110879895	*NPHP1*	loss
1207	2	g.110879716	g.110962709	*NPHP1*	loss

[a] Based on the GRCh37 assembly

Supplementary Table S4. Mutations in the genes related with nephronophthisis

Patient	Mutation	Gene [a]	cDNA change	Protein change	Mutation type	CADD	Polyphen	SIFT	ExAC	ToMMo	Previous reports
720	Frameshift	*NPHP3*	c.2425dupA	p.M809fs	Heterozygous	None	None	None	None	None	None
	Missense	*NPHP3*	c.2171G>A	p.R724H	Heterozygous	4.99	0.001	0.6	None	None	None
478[b]	Missense	*NPHP4*	c.2198G>A	p.G733D	Heterozygous	20.1	1	0	9.10E-05	0.0037	None
	Missense	*NPHP4*	c.2717G>A	p.R906H	Heterozygous	5.89	0.003	0.21	0.0002	0.0061	None
1107	Nonsense	*NPHP1*	c.1639C>T	p.Q547*	Homozygous	38.0	None	None	None	None	None
930[b]	Missense	*CEP164*	c.3737G>A	p.R1246Q	Heterozygous	3.32	0.001	0.65	8.24E-06	0.0005	None
	Missense	*CEP164*	c.452G>A	p.R151Q	Heterozygous	24.6	0.999	0.0	4.12E-05	0.0049	None

CADD, combined annotation-dependent depletion; SIFT, sorting intolerant from tolerant; ExAC, exome aggregation consortium; ToMMo, Tohoku Medical Megabank Organization

[a] The following NCBI reference sequences were used: *NPHP3*, NM_153240.4; *NPHP4,* NM_015102.4; *NPHP1*, NM_000272.3; *CEP164*, NM_014956.4

[b] Patient numbers 478 and 930 were confirmed compound heterozygous mutations by trio analysis

Supplementary Table S5. Clinical characteristics of the pathologic control group

Age[a]	Sex	eGFR[a], mL/min/1.73 m^2	Pathologic diagnosis	Percentage of tubulointerstitial fibrosis
42	M	30.1	IgA nephropathy	30–40%
49	M	26.0	IgA nephropathy	30–40%
54	M	33.3	Diabetic nephropathy	N.D.
63	M	19.5	Tubulointerstitial nephritis	30%
63	F	30.0	Tubulointerstitial nephritis	10%
68	M	15.7	Diabetic nephropathy	80–90%
70	F	33.8	IgA nephropathy	30%
74	M	86.0	Diabetic nephropathy	20%
80	M	20.0	IgA nephropathy	30%

M, male; F, female; N.D., no data

[a] At the time of renal biopsy

Supplementary Figure 1. Representative pathologic findings

a. Tubular diverticulum (patient number 914, PAM stain, 20× magnification). b. Tubular floret, which is defined as branching in at least four directions (patient number 742, PAM stain, 20× magnification). c. Cyst, which is defined as >200 μm in diameter (patient number 742, PAM stain, 10× magnification). All slides were scanned on a NanoZoomer NDP system with 40× resolution (0.23 μm/pixel) (Hama-matsu Photonics, Hamamatsu-City, Japan).

PAM, periodic acid methenamine silver

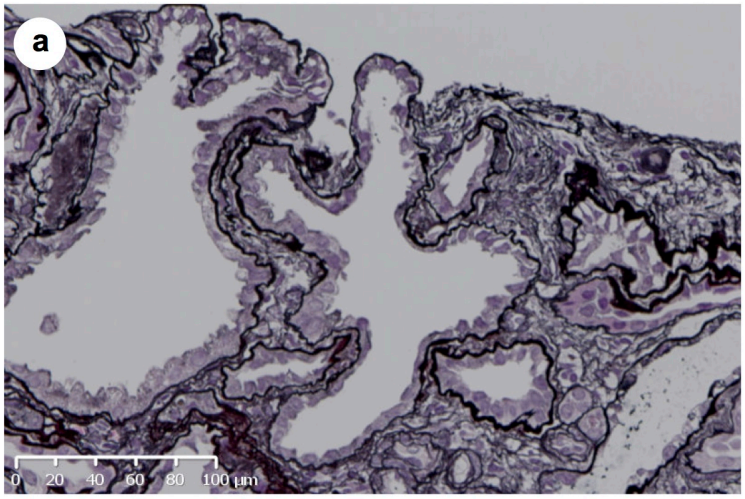
a
0 20 40 60 80 100 µm

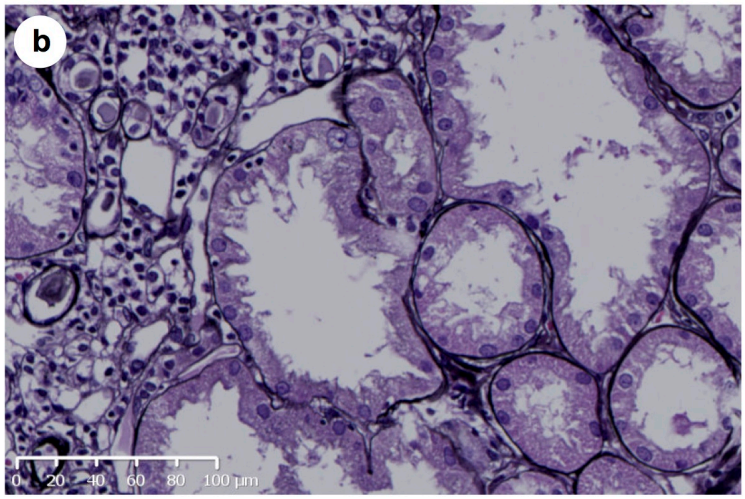
b
0 20 40 60 80 100 µm

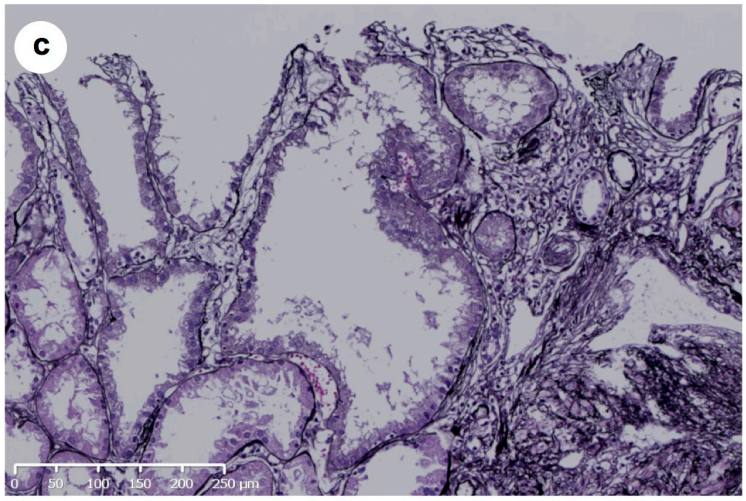
c
0 50 100 150 200 250 µm